NGU REPORT

**Rare earth elements (REE) in two long
drill-cores from the Fen Carbonatite
Complex, Telemark, Norway**

NORGES GEOLOGISKE UNDERSØKELSE
- NGU -

REPORT

Report no.: 2019.008	**ISSN:** preliminary version **ISSN:**	**Grading:** open

Title: Rare earth elements (REE) in two long drill-cores from the Fen Carbonatite Complex, Telemark, Norway (preliminary version)

Authors: Nolwenn Coint and Sven Dahlgren	**Client:** Government
County: Telemark	**Commune:** Nome
Map-sheet name (M=1:250.000) Skien	**Map-sheet no. and -name (M=1:50.000)** 1713-4 Nordagutu
Deposit name and grid-reference: Fen Complex	**Number of pages:** **Price (NOK):** **Map enclosures:**

Fieldwork carried out:	**Date of report:** 28/02/2019	**Project no.:** 379500	**Person responsible:**

Summary:

Rare Earth Elements (REE) are metals that are classified as critical for the European industry. They are fundamentally important in the manufacturing of HiTech and green technology products. Today almost the total world REE-mining is controlled by China. REE deposits in Europe are few and none of them are in production. The Fe-dolomite carbonatites ("rauhaugites") in the Fen Carbonatite Complex in Telemark, Norway, has for some years been known to host abundant REE-minerals. The knowledge of this rock type has, however, been limited to the near surface environment. In 2017 the Ministry of Trade, Industry and Fisheries funded a reconnaissance core-drilling program to test the continuation of the Fe-dolomite carbonatite at depth. Two rock cores, 1001 and 716 metres long, were recovered at the drill-sites, LHKB-1 (near Fen old school) and LHKB-2 (east of Søve) respectively. Core LHKB-1 consists almost only of Fe-dolomite carbonatites down to 1001 metres depth. Core LHKB-2 also consists of Fe-dolomite carbonatite from top to bottom, but cross-cutting damtjernites (a lamprophyric rock) occur in some intervals. Scattered REE-mineralizations are abundant in both drill-cores. Rare Earth Element-minerals are REE-fluorocarbonates (bastnaesite, parisite-synchysite), and subordinate REE-phosphate (monazite). The LHKB-2 core is generally richer in REE (median TRE_2O_3 1.70 wt%) than the LHKB-1 (median TRE_2O_3 1.08 wt%). The thorium content is low (median 181.5 and 128.5 ppm in LHKB-1 and 2 respectively) in these Fe-dolomite carbonatites compared to the Fen rødbergite. Geological, hyperspectral and geochemical analyses of these two reconnaissance drill-cores demonstrates that the REE-bearing Fe-dolomite carbonatites extend at least down to a depth of 1000 metres. An industrial exploration program of the Fen Complex should be considered. This report with appendices presents all chemical and hyperspectral data available from these two reconnaissance cores, and thus serves as an excellent basis for competent industry to plan an eventual exploration program.

Keywords:	Fen Complex	Rare Earth Elements
Rauhaugite	Fe-dolomite carbonatite	Hyperspectral imaging
Whole-rock analyses		

CONTENTS

FIGURES

TABLES

APPENDICES

Appendix 1 : Drill site geological work

Appendix 2 : Hyperspectral imaging method

Appendix 3 : Whole-rock geochemistry method

ENCLOSURES

Enclosure 4.1: RGB photos of cores

Enclosure 4.2 : Hyperspectral data

Enclosure 4.3 : Geochemical data

1. INTRODUCTION

Carbonatite and alkaline intrusive rocks are the primary source for Rare Earth Elements (REE) consisting of 15 chemical elements, the lanthanides (Lanthanum, [57]La to Lutetium, [71]Lu), Yttrium ([39]Y) and Scandium ([21]Sc). Rare Earth Elements can be divided into two groups, Light Rare Earth Elements (LREE) and Heavy Rare Earth Elements (HREE), based on their atomic mass (Fig. 1). Rare Earth Elements, which share very close geochemical characteristics, tend to be enriched by similar chemical processes and are therefore often found together in rocks such as carbonatites. However, the REE's display various metallurgical, catalytic, chemical, electrical, magnetic and optical properties and are therefore used for a wide range of industrial applications (Fig. 2).
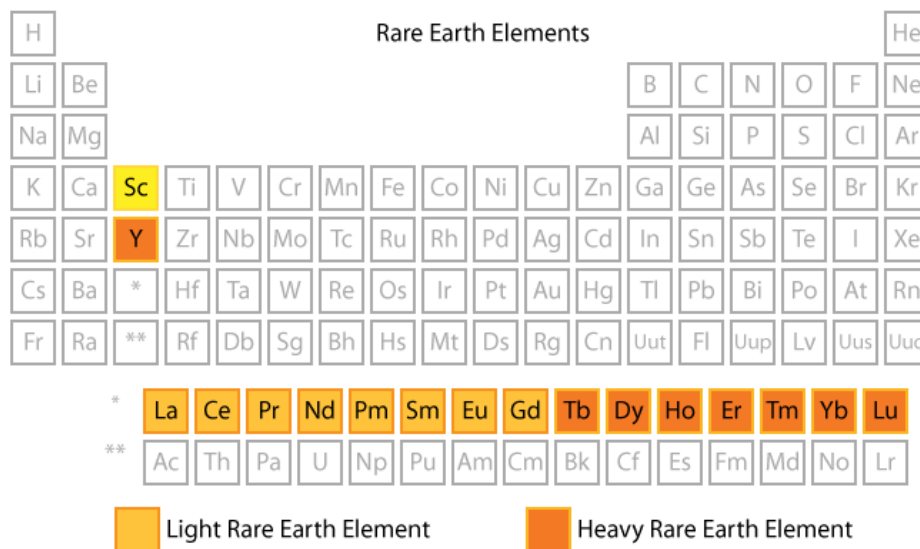
Figure 1: Periodic table of elements. Rare Earth Elements are highlighted in orange.

While REE's are not actually rare in nature, exploitable concentrations are uncommon. As of 2014, only six deposits around the world were actively mined, all of them in carbonatites: Bayan Obo, Daluxiang, Maoniuping and Weishan in China, Mount Weld in Western Australia and Mountain Pass in California (Verplanck *et al.*, 2014). Despite the diversity of REE-minerals, REE are extracted from only three REE-minerals: bastnäsite, monazite, both enriched in LREE and xenotime, enriched in HREE (Verplanck *et al.*, 2014).

Rare Earth Elements are important components for the development of new technologies (Fig. 2). They are used both by the industry (ceramics and glass, oil refining, metal alloys, different types of lasers, batteries, permanent magnets) but also in new technologies used in modern society on a daily basis, such as smart phone and tablet screens. They play a crucial role in the transition to de-carbonised society through the development of permanent magnets for wind turbine and batterie used in electric cars. As a result, the demand for these elements is increasing.
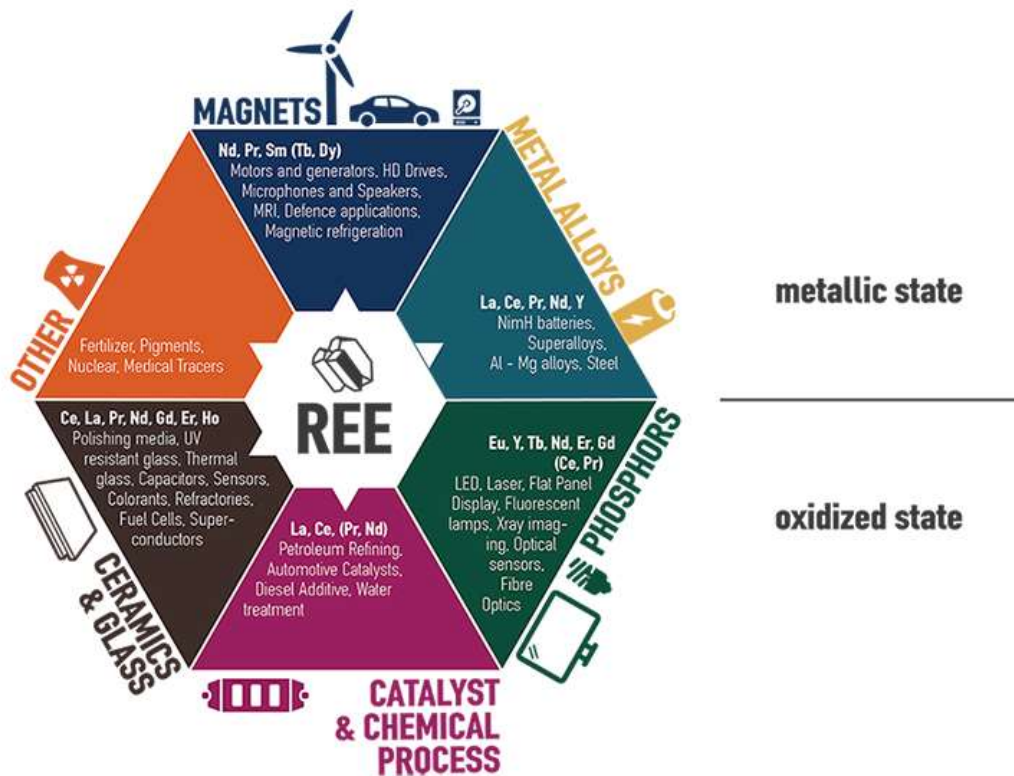
Figure 2: Rare Earth Elements usage in various technologies
(http://www.eurare.eu/RareEarthElements.html)

Since the mid-eighties, China has increased its production of REE, to attain 95% of the world production in 2012 (Tse, 2011), whereas the US saw their production stop in 2002 when the Mountain Pass mine closed (Fig. 3).

The pseudo-monopoly of China within REE production and its tactical decision to limit its REE export lead to a crisis in mid-2011, when the prices for Rare Earth Oxides (REO) reached a record high.
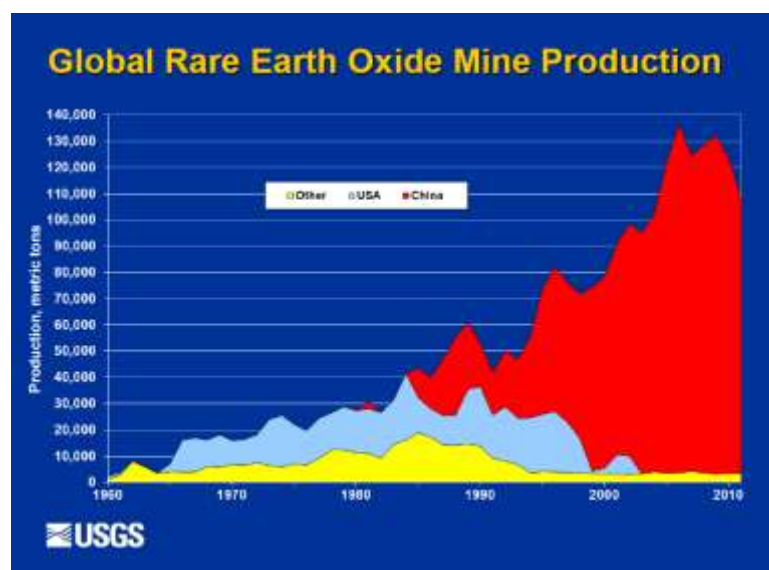
Figure 3: Global Rare Earth Oxide (REO) production.
https://minerals.usgs.gov/minerals/pubs/commodity/rare_earths/ree-trends-2010.pdf

This crisis lead to a strong effort to characterize and map potential REE resources (Paulick & Machacek, 2017), and the rare earth elements are now listed as critical in several countries and continents (USGS, 2011). Many important EU industry companies are dependent on REE's for the manufacturing of a variety of products. However, the EU is totally dependent on the import of REE. Several evaluations of the criticality of raw-materials in the EU, including the last criticality assessment in 2017 (http://ec.europa.eu/growth/sectors/raw-materials/specific-interest/critical_en), classify the REE's as the elements with the highest supply-risk of any commodity.

Accordingly, the EU-project "EURARE", was implemented in 2013 with the aim, amongst other topics, to assess known REE deposits in Europe, and their potential for future supply of REE raw materials to the European markets. This project was completed in 2017 (http://www.eurare.eu/docs/T1.1.2_Report-final-280217.pdf). The Fen Carbonatite Complex was described as one of the European deposits having a future potential. However, comparably little modern information on the geology and distribution of REE's was available from the complex during the EURARE project.

In 2017, the Norwegian Ministry of Trade, Industry and Fisheries funded two deep drill holes in the Fe-dolomite carbonatite (rauhaugite) of the Fen Complex, the largest potential REE deposit of the country (http://www.eurare.eu/countries/norway.html), to characterize the REE-minerals, their distribution and textural relationships.

The drilling performed cannot be considered exploration drilling. The drill-cores were extracted in order to confirm a geological model of importance to future REE exploration.

Two drill-sites were chosen (see appendix 1 for details), and both were drilled vertically:
LHKB-1: Located on a grain-field about 80 metres WSW of the old, abandoned Fen school. Drilled to 1001.3 m depth.
LHKB-2: Located on a cattle-field about 200 metres ESE of the Søve agricultural school. Drilled to 716.4 m depth.
LHKB = Langhullskjerneboring (= "long-hole core-drilling").
The two drill-sites were located about 903 metres apart (appendix 1).

Success criteria
Two success criteria were formulated for the drilling project:
- The major goal of the drilling was to confirm the downwards extent of the Fe-dolomite carbonatite. If the Fe-dolomite carbonatite were found down to 1000 metres, then drilling would prove that a rock type which may host REE-mineralizations has considerable volume within the Fen Complex.
- Another important, but subordinate, question was whether there were traces of REE-mineralizations in the cores.

The results presented in this report shows that the answer to both these questions are "YES".

In this report we present results from
- Geological observations
- Hyper-spectral core-logging and analysis
- Whole-rock geochemistry

The results presented in this report provide important information important for the consideration of future REE exploration in the Fen Complex. Additional information is available in the appendices and enclosures.

2. The Fen Carbonatite Complex

The Fen Complex (Fig. 4) is a circular carbonatite and alkaline complex of about 4-5 km^2 (Goodenough *et al.*, 2016), emplaced around 580 million years ago in Mesoproterozoic orthogneisses in the Telemark county, Southern Norway (Dahlgren, 2004). It is located south of Lake Norsjø and east of the village of Ulefoss The emplacement of the complex was contemporaneous with a widespread alkaline fluid-related alteration of the surrounding rocks called "fenitization"(Andersen, 1989).
The complex most likely represents the roots of a totally eroded volcano (Brøgger, 1921, Dahlgren, 2006). Gravity modelling suggests a cylindrical downwards continuation to at least 14 km depth (Ramberg 1973).
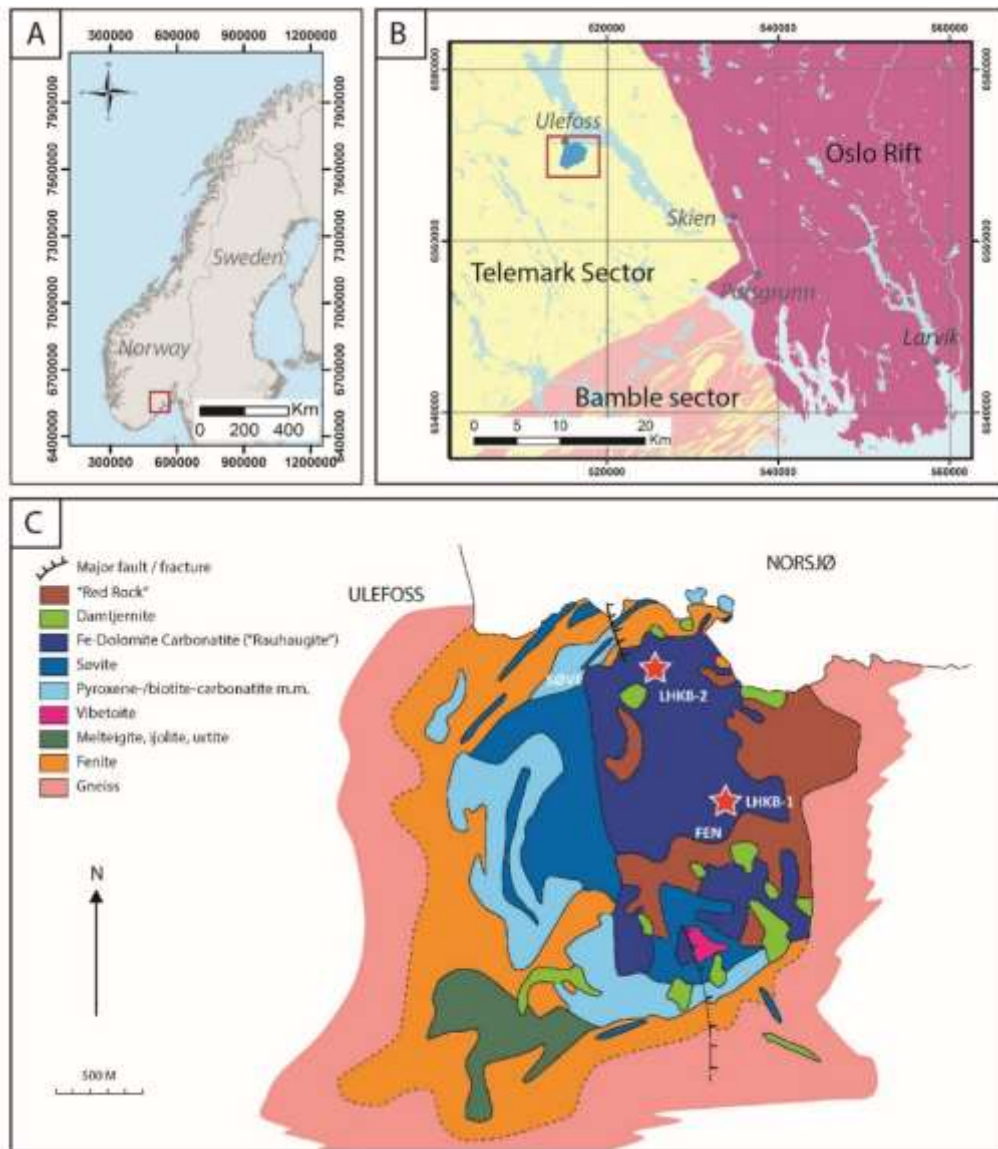
Figure 4: Simplified geologic map of the Fen Complex. A. Location of the Fen Complex in Norway. B. Simplified geologic map of the area (NGU 1:250 000 harmonized bedrock database). C. Simplified geological map of the Fen Complex.

Brøgger (1921) described a large variety of magmatic and metasomatic rocks within the Fen Complex. These included alkaline silicate rocks, carbonatites and mixed silicate-carbonate rocks, all regarded by Brøgger as magmatic. He named the various rocks after local farms. He also recognized a strong alkali-metasomatism of the gneisses adjacent to the alkaline silicate rocks and some of the carbonatites, and he introduced the name "fenite" for such alkaline metasomatic rocks, and the tern "fenitization" for the process of their generation. The magmatic rocks were formed by numerous magma pulses. The rough sequence of events was established by Brøgger, and later modified by Sæther (1957). The sequence of events is currently being further modified (Dahlgren in prep), and the main stages are as follows:

1. Intrusion of alkaline silicate magmas producing rocks consisting of various proportions of the major minerals, clinopyroxene (aegirine-augite to aegirine), nepheline and K-feldspar. Rocks formed are melteigite, ijolite, urtite and nepheline syenite among others. Fluids that escaped from the magmas produced fenites

10

characterized by aegirine and alkali amphiboles. Associated carbonatites were clinopyroxene-calcite carbonatites (by some workers termed "silicocarbonatites").

2. Intrusion of søvites (calcite carbonatites) and rauhaugites (dolomite carbonatites). The søvites typically contain apatite, phlogopite, amphibole, magnetite and pyrochlore. The dolomite carbonatites consist of a Fe-poor dolomite with a variable, but generally low apatite content. These dolomite carbonatites were termed rauhaugite type 1 by Sæther (1957).

3. Formation of rauhaugite type 2 characterized by a dolomite richer in Fe than the type 1 rauhaugites (Sæther, 1957). This is an important distinction not made by Brøgger (1921), and as type 1 and 2 are quite different rocks the term "rauhaugite" should not be formally used. The rauhaugite type 2 has also been termed "ferrocarbonatite" (Andersen, 1986, Andersen, 1987), but this term also has drawbacks. The typical carbonate is, however, Fe-dolomite, and thus the term "Fe-dolomite carbonatites" is preferred (Dahlgren in prep). This term is used in this report, and it is within this unit the LHKB-1 and LHKB-2 cores were drilled.

4. Intrusion of damtjernite, a group of mixed silicate-calcite rocks characterized by megacrysts of Ti-phlogopite (Brøgger, 1921, Sæther, 1957). This rock is typically strongly altered to chlorite-carbonate rocks within the Fen Complex, but most commonly their phlogopite megacrysts are still easy to recognize. At least some of the damtjernites are mantle-derived (Dahlgren, 1987, Dahlgren, 1994, Griffin, 1973).

5. Generation of "red-rocks" (= rødbergite). This is a hydrothermal alteration, i.e. hematitization, product of older Fen-rocks (Andersen, 1984, Brøgger, 1921, Sæther, 1957).

The geology of the Fen Complex is presently being re-mapped (2015-2019) and will be described and re-interpreted in more detail in subsequent reports and papers (Dahlgren in prep).

Core_ID	Location	Northing	Easting	Depth to bedrock (m)	Length (m)
LHKB-1	W of Fen old school	6570373.2	517182.7	13.24	988.06
LHKB-2	E of Søve agricultural school	6571021.5	516554.7	4.9	711.5

Table 1: GPS coordinates of the two reconnaissance cores (WGS1984 UTM zone 32).

Mining of different commodities has previously been carried out within the Fen Complex. Iron mines were operated from the 1650s to 1927 on hematite ores within the "rødbergite" (Dahlgren, 2006, Sæther, 1957, Vogt, 1918). Søvite was mined for niobium in the period 1953 to 1965 .

The Fen Complex also hosts a thorium mineralization of global significance. The thorium is confined to the "red-rocks" and the Fe-dolomite carbonatites (Dahlgren, 1983, Dahlgren, 2008, Dahlgren, 2012, Dahlgren, 2015, Heincke et al., 2008, Svinndal, 1973). However, the thorium content of the Fe-dolomite carbonatites is generally much lower than in the rødbergite (Dahlgren 2012, 2015). Although the "red-rocks" contain a substantial amount of REE's, benefication of REE's from this rock type has proven to be difficult (Svinndal, 1971),

and the rødbergite must be considered a less promising exploration target at present. However, research is still going on with hydrometallurgical studies of the rødbergite (Davris et al., 2018). Currently the Fe-dolomite carbonatites represent the major exploration target within the Fen Complex (www.reeminerals.no) (Dahlgren, 2015).

3.   Work performed

Down-hole geophysical measurements, including total gamma ray and individual measurements for U, Th and K, electromagnetic properties, sound velocity, resistivity and data from optical tele viewer, were acquired once the drilling was finished, in April 2018. Results of these investigations will be presented in a subsequent report.

Both drill-cores were systematically cleaned, photographed and logged (see Appendix 1). The cores were then split in two at the core storage facility at the Geological Survey of Norway. The half drill-core is stored at NGU for reference, whereas the second half was split into two quarter cores. One quarter of the core was used for whole-rock geochemistry.

Both hyperspectral imaging and whole-rock chemistry were conducted systematically. The hyperspectral imaging method is presented in Appendix 2, whereas the method for geochemical analyses is presented in Appendix 3.

4.   RESULTS

4.1 Geological observation

Red Blue Green "standard" photos were also taken of all core-boxes during the Hyperspectral scanning. These photos are displayed in Enclosure 4.1

4.1.1   <u>What is Fe-dolomite carbonatite (rauhaugite)?</u>

The LHKB-1 and LHKB-2 cores were drilled in "rauhaugite", or "Fe-dolomite carbonatite". From observations made at field-exposures, of new shallow cores, of old exploration-cores, within old mine-workings and in these two long cores, it is evident that "rauhaugite type 2" or "Fe-dolomite carbonatite" is not a single rock-type. At best, the rocks, here referred to as "Fe-dolomite carbonatite", can be described as a rock group which embrace a lot of texturally different-looking rock varieties, and with colours varying from very dark gray to very light gray or pinkish-/yellowish gray. The colour differences mainly reflect modal variations of light and dark minerals. Typically, the grain-size varies from fine to very fine-grained, although medium, coarse and very coarse-grained varieties do occur.

So far limited detailed mineralogical work has been performed on the rocks from the LHKB-1 and LHKB-2 cores. However when thin sections become available more mineralogical details will emerge.

4.1.2 <u>LHKB-1 lithology</u>

A large part of this core consists of "Fe-dolomite carbonatites". They show a great variety of textures (Fig. 5), but can very roughly be subdivided into:

Breccias. Many textural varieties of breccias and breccia-like rocks dominate the entire core (Fig. 5 B, C and E). Variable modal proportions of chlorite and carbonate causes colour differences. REE-minerals may occur in veins, disseminated grains or in cm-sized clusters. In some breccias no REE-minerals are visible without a microscope.

Laminated type. Gray-coloured and very fine to fine-grained type with mm to cm spaced laminae occurs in several intervals below 476 m. Rare Earth Element-minerals are very fine-grained when they have been observed with hand-lens. A typical texture is shown in figure 5F.

Granular type. This type is usually of pink colour and fine- to medium-grained (Fig. 5A). It can contain REE-mineral clusters up to 1 cm or more (Fig. 5D) and is typically rich in sulfides (pyrite/pyrrhotite).

Chlorite-rich rocks constitute the deepest level rocks (below ca 960 m) of the core. They are dark-coloured and very heterogeneous. Some look like deformed mafic breccias, e.g. figure 5G from the base of the entire core. These rocks may represent rocks in the "dense body" modelled from gravity (Ramberg 1973).

Probable xenoliths. Chlorite-rich domains (e.g. at levels 35 m, 56 m etc) may represent highly altered mafic silicate rocks. Søvite xenoliths occur at several intervals, e.g. at 883.6 to 884 m.

Rødbergite represents a hydrothermal alteration zones rich in hematite. They are confined to shallow depths, e.g. at 22.5-25 and 146 m.

Apatite-rich domains/veins, REE-mineral clusters, sulfide clusters, fluorite-rich zones, barite enriched pods and magnetite-apatite veins occur at many places throughout the core.

Damtjernite. Only a couple of small highly altered damtjernite dykes occur at 318 and 341 m. Other highly altered, mafic/ultramafic dykes also occur in the lowermost parts of the core.

Dolerite dyke. This is the ordinary dark gray dyke-rock, common in the Oslo rift. It consists of altered plagioclase and dark minerals. Similar dykes are cutting across the Fen Complex in numerous localities (Brøgger, 1921). Three sheets occur in the interval 204.9 to 209.7 m.

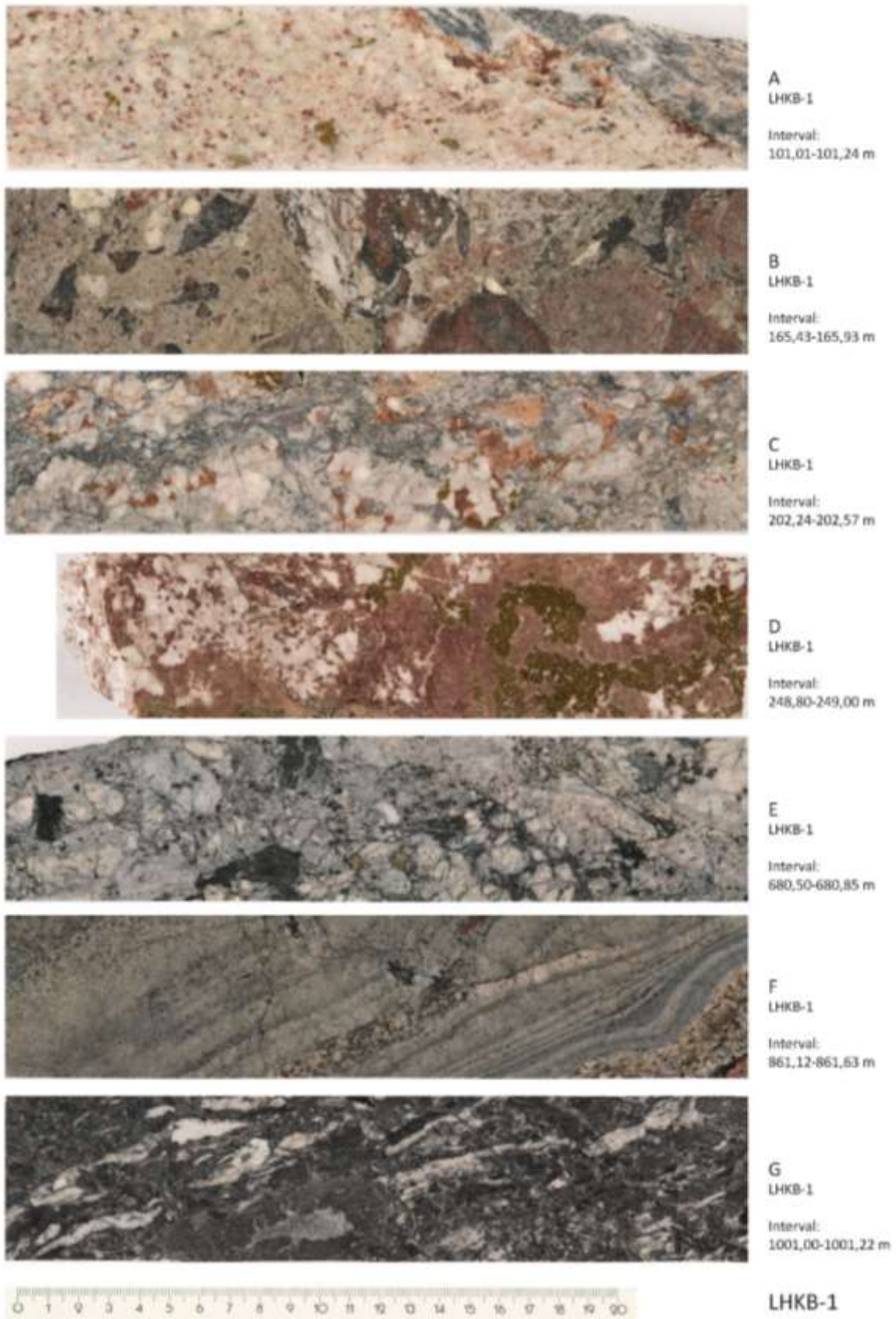*Figure 5: Macro-photos illustrating the variety of textures encountered in LHKB-1. A. Granular carbonatite with mm-sized REE-mineral clusters (red) and sulfide clusters up to 1 cm. B. "Barren" breccia. C. Breccia with abundant (red) REE-mineral clusters. D. A large REE-mineral cluster with large sulfide domains. E. Breccia with scattered small REE-mineral clusters. F. Laminated carbonatite. G. Chlorite-rich rock.*

4.1.3 <u>LHKB-2 lithology</u>

In the LHKB-2 core damtjernite is occupying large intervals, which makes a distinct difference between this and the LHKB-1 core. Otherwise the Fe-dolomite carbonatites also dominates LHKB-2.

The Fe-dolomite carbonatite in LHKB-2 shares many characteristics with the Fe-dolomite carbonatite of LHKB-1 such as the presence of breccias (Fig. 5B, C &E), but there are also some textural differences (Fig. 6 A-C & F). Some of the Fe-dolomite carbonatite in this core displays a characteristic planar texture (Fig. 6B), a foliation which most likely was formed by deformation of a Fe-dolomite carbonatite breccia. The REE-minerals are fine-grained and dispersed through the rock.

Damtjernite occurs at many intervals in the LHKB-2 core and is especially abundant in the intervals 51.5 to 122 m, 226 to 250 m, 325 to 450 m and 498 to 514.5 m. The damtjernite typically contain angular xenoliths of søvite and Fe-dolomite carbonatite (Fig. 6D & E), i.e. the damtjernite is younger than these two rock types. The damtjernite minerals, e.g. former clinopyroxene, olivine etc are strongly chloritized and carbonatized. Even phlogopite megacrysts, which typically have survived in many other damtjernites in the Fen Complex, are strongly altered.
The drilling was stopped at 716.4 m at this site due to technical problems. The core from 716.3 m is displayed in figure 6G. The rock is interpreted as a deformed and carbonatized breccia which originally contained mica phenocrysts, but which is now completely chloritized.

A **dolerite** dyke is also found in this core at 140.1 to 141.5 m.

In summary the rocks of the two drill-cores LHKB-1 and LHKB-2 are extremely heterogeneous although most of them are called Fe-dolomite carbonatite. The REE-mineral clusters are also heterogeneously distributed, whereas tiny REE-mineral grains apparently are more "evenly" dispersed within the entire rock volume.
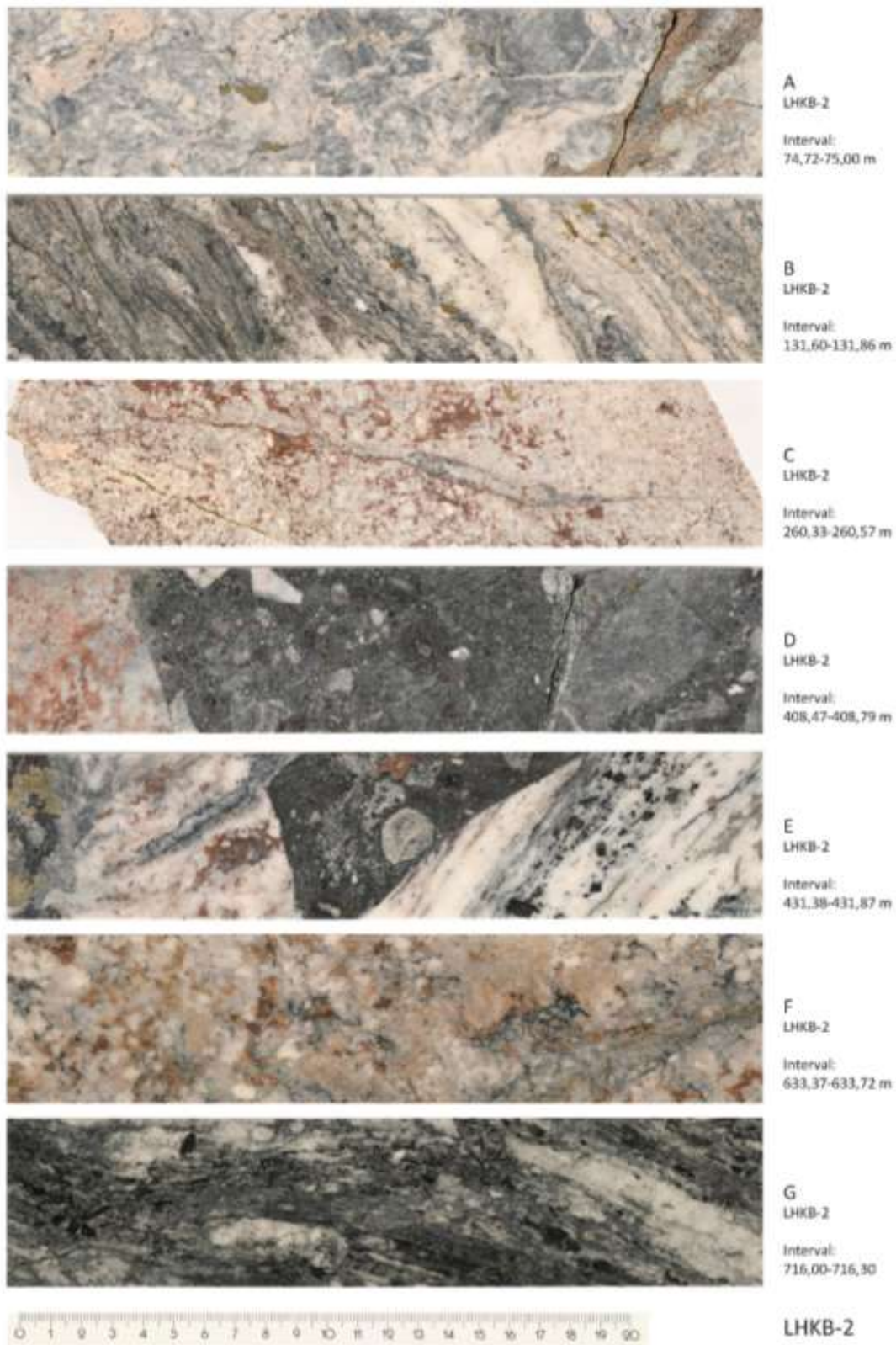
Figure 6: Macro-photos illustrating the variety of textures encountered in LHKB-2. A. Light-coloured Fe-dolomite breccia with REE-minerals-rich vein on the right side of the photo. B. Characteristic planar texture of Fe-dolomite carbonatite. Note the fine-grained dispersed REE-minerals. C. Granular Fe-dolomite carbonatite with REE-mineral clusters (red). D. Damtjernite (dark gray) containing angular xenoliths. E. Damtjernite (dark area in the middle) containing an angular søvite xenolith (right side) and a Fe-dolomite carbonatite (left side). F. Fe-dolomite carbonatite rich in REE-mineral clusters. The texture is transitional between a granular type and a breccia. G. Deformed carbonatized breccia.

16

4.2 Hyperspectral scanning

The principle and method of hyperspectral imaging are described in Appendix 2.

4.2.1 Core logging using LWIR data

As illustrated in the previous section, carbonatites display complex textural relationships at the metre- to micrometre scale (Enclosure 4.1 and Fig. 5 & 6), which makes consistent logging complicated. Simplified logs for both cores and their respective interpreted lithology logs, based on dominant minerals identified using the LWIR hyperspectral data (Enclosure 4.2), are presented in Figure 7. In this figure different types of carbonatite are not distinguishable.

Four main lithologies can be identified using the hyperspectral data. Carbonatite is the main lithology. It makes up most of LHKB-1 (Fig. 7). Even though Fe-dolomite carbonatite dominates, minor amount of rødbergite is also present. The second lithology distinguishable with the LWIR data is the apatite-rich rocks, also known as phoscorites (Krasnova *et al.*, 2004). They form centimetre to tens of centimetre-thick layers. Scarce intervals rich in quartz and barite are also noted. A 4.5 m-thick dolerite dyke, related to the formation of the Oslo Rift during the late Carboniferous-Permian ages cuts the older Fen Complex between 205 and 210 m.

The second core, LHKB-2, is also dominated by carbonatite. The latter, however, is brecciated in many areas by damtjernite, resulting in a larger amount of chlorite in the core (Fig. 6D & E, Fig. 7). As in LHKB-1, thin centimetre- to tens of centimetre-scale apatite-rich layers are also common. Some of them are associated with damtjernite (335.5 to 447.8 m and 698.2-716.4 m). A dolerite dyke (140 to 141.5 m) cuts the carbonatite.
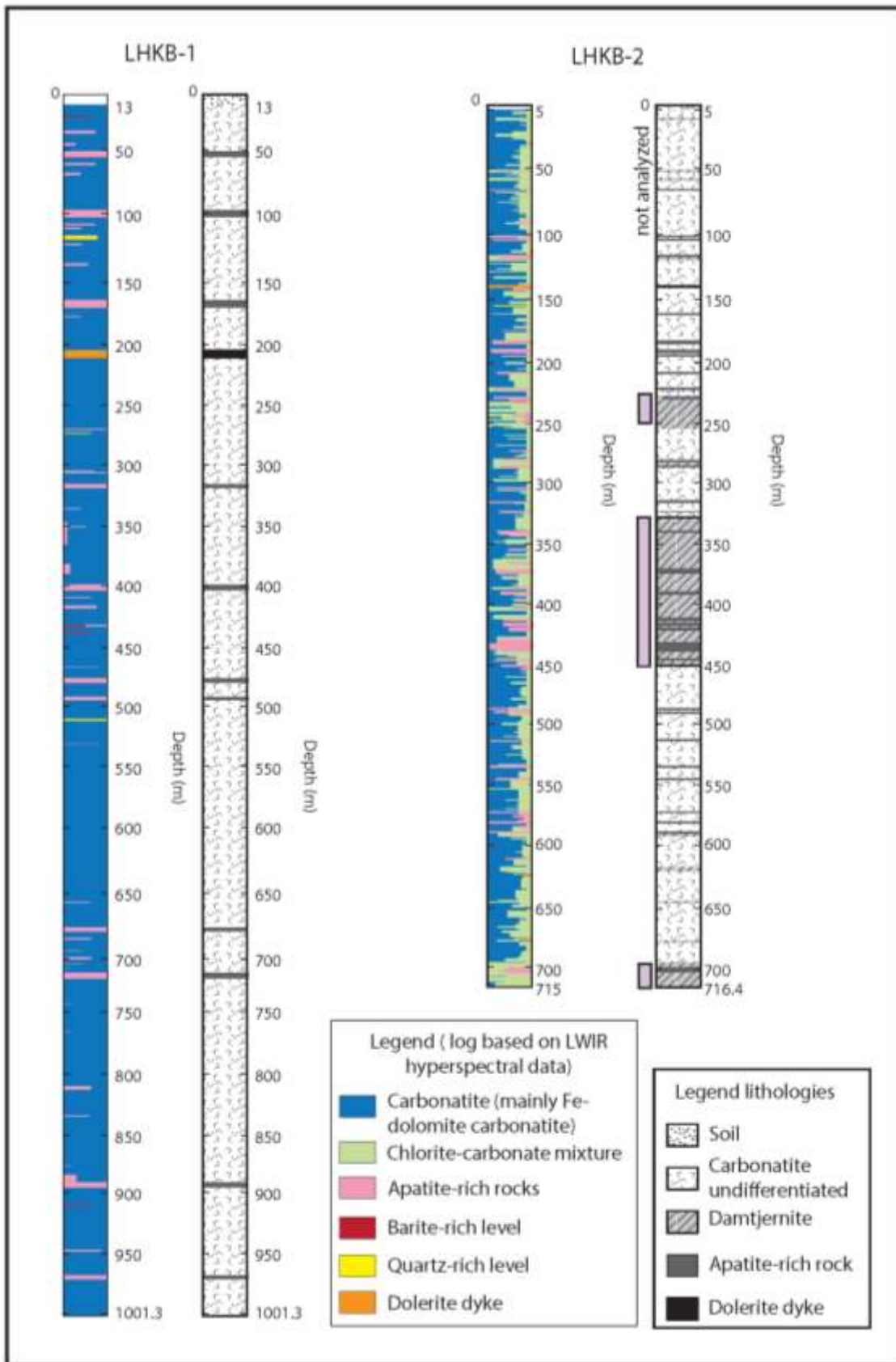
Figure 7: Simplified logs based on dominant minerals extracted from hyperspectral data (LWIR).

4.2.2 Processed hyperspectral images

Several interesting features, regarding the amount of carbonate present in the cores, their composition but also the amount of apatite and the location of the largest REE-mineral clusters, were extracted from the hyperspectral dataset and can be found in Enclosure 4.2. Each data processing step and keys to reading the resulting images are briefly described below.

File Name	Core	Content description	Camera	File
LHKB-1_DominantMineral	LHKB-1	Automatic generated logs (LWIR data)	LWIR	PDF
LHKB-2_DominantMineral	LHKB-2	Automatic generated logs (LWIR data)	LWIR	PDF
LHKB-1_ListBoxes	LHKB-1	box and sample numbers		XLS
LHKB-2_ListBoxes	LHKB-2	box and sample numbers		XLS
CarbIntensity-LHBK-1	LHKB-1	carbonate intensity	LWIR	PDF
CarbIntensity-LHBK-2	LHKB-2	carbonate intensity	LWIR	PDF
CarbCompo-LHBK-1	LHKB-1	carbonate composition	LWIR	PDF
CarbCompo-LHBK-2	LHKB-2	carbonate composition	LWIR	PDF
ApIntens-LHBK-1	LHKB-1	apatite intensity	LWIR	PDF
ApIntens-LHBK-2	LHKB-2	apatite intensity	LWIR	PDF
Grid800-LHBK-1	LHKB-1	Grid D800, enhance REE-minerals	VN-SWIR	PDF
Grid800-LHBK-2	LHKB-2	Grid D800 enhance REE-minerals	VN-SWIR	PDF

Table 2: List of files available in Enclosure 4.2 and short description of their content.

4.2.2.1 Carbonate intensity (LWIR)

The carbonate intensity parameter reflects the strength of the spectral signature related to the presence of carbonates and is a qualitative way to quantify the amount of carbonate in the rock. The warmer the colour, the more carbonate there is.

4.2.2.2 Carbonate composition (LWIR)

Carbonate minerals display a large peak between 11000 nm and 11400 nm (LWIR) (Fig. 8). The position of this peak is a function of the carbonate chemistry. By colour-coding the variation of the peak position, qualitative variations in the chemistry of the carbonate throughout the cores can be assessed.
The more Mg-rich the carbonate, the shorter the wavelength of the main peak (Fig. 8C).
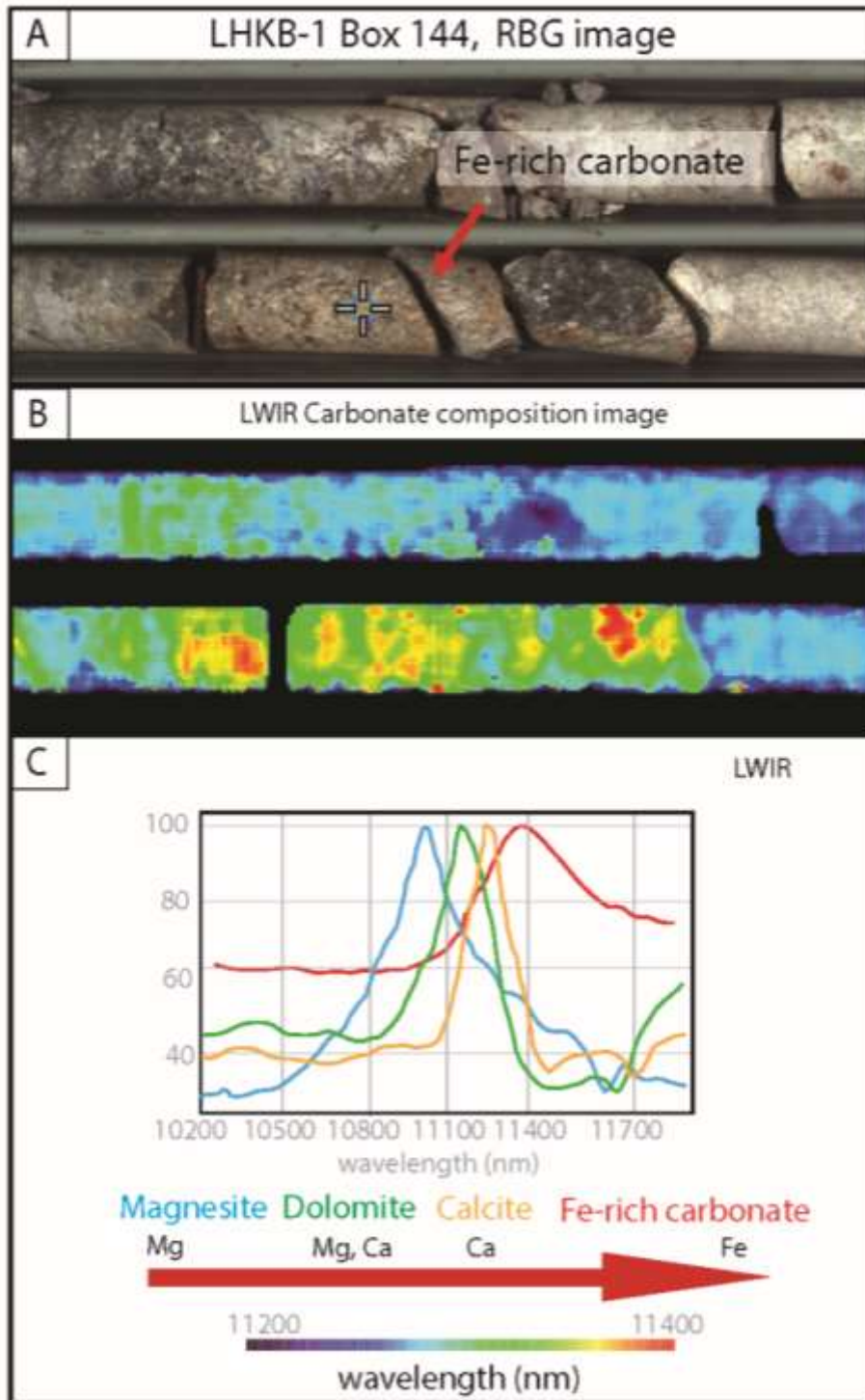
Figure 8: Carbonate compositional variations illustrated by LWIR data. A. Fe-rich carbonate (probably ankerite) in LHKB-1 core. B. LWIR carbonate composition image of the same area. C. Spectra of different carbonates encountered in carbonatite.

In the Carbonate Composition dataset, the warmer the colour, the more Fe-rich the carbonate (Fig. 8B).

4.2.2.3 Grid D800 and location of the REE-mineralizations

Rare Earth Element-bearing minerals are not always coarse enough to be spotted in the hyperspectral data. However, locally, they occur as clusters which can reach several centimetres. Recent studies have demonstrated that REE-minerals display a series of tight peaks and troughs between 500 and 900 nm (VN-SWIR dataset), related to the presence of Nd in the mineral(red arrows in Fig. 9) (Neave *et al.*, 2018, Turner *et al.*, 2014).
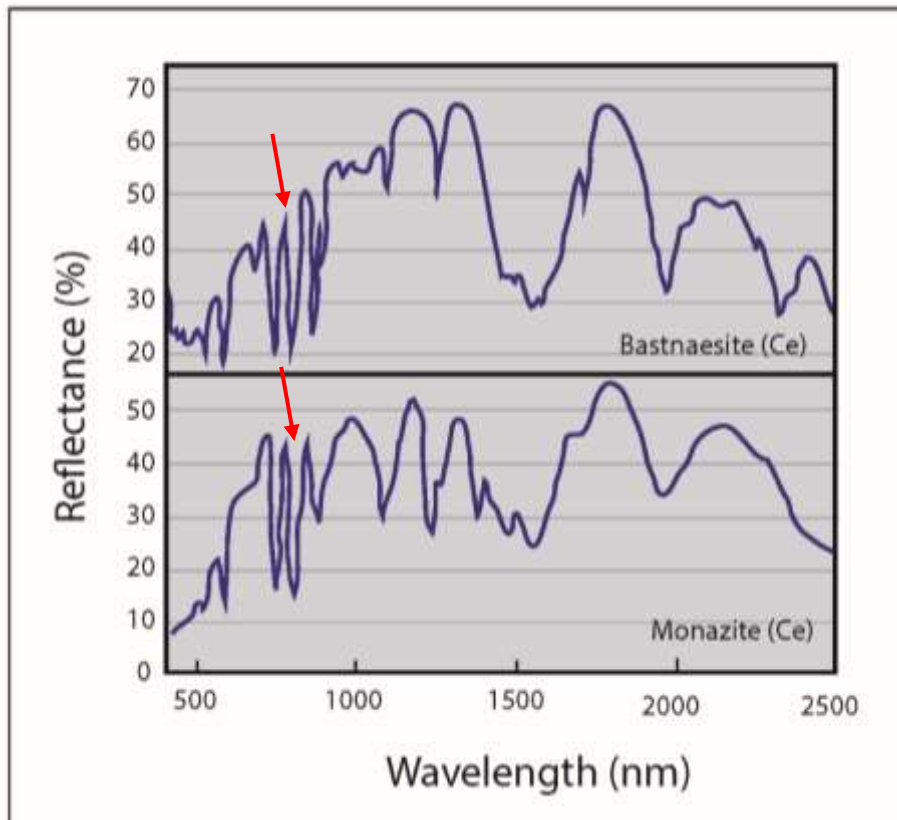

Figure 9: Reflectance spectra of REE-minerals encountered in carbonatite.

These characteristic abortion features can be enhanced and filtered from the hyperspectral data to spot the location of large LREE-minerals clusters.

The hyperspectral dataset was filtered to enhance one of these Nd-related troughs (Fig. 9 & 10). The Hull Quotient method which consists of removing the background from the spectra in order to enhance the troughs observed in the reflectance spectra (Fig. 10 C) was applied to the dataset. Grid D800 represent the depth of the trough observed after such a treatment of the data. The warmer the colour, the higher the content of LREE-bearing mineral in the core.
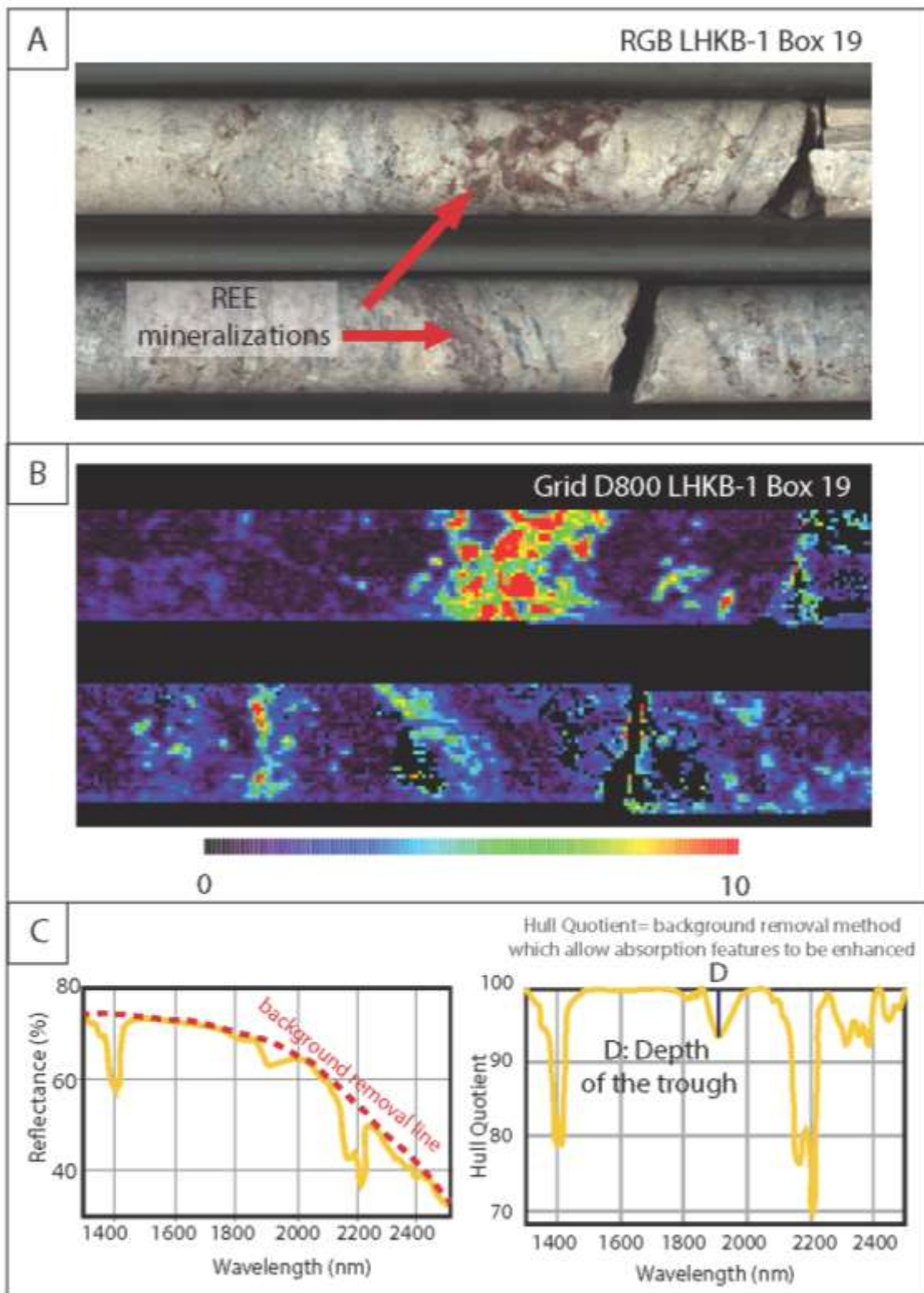
Figure 10: Grid D800 enhancing REE-minerals-related features. A. RGB photo of the core showing a zone enriched in REE-bearing minerals. B. Grid D800 image of the same part of the core as in A. C. Reflectance spectra and hull quotient background removal method (see text for explanation).

4.2.2.4 Apatite intensity

The same principle as for carbonate intensity can be used for apatite. Apatite, a primary source for phosphorous for fertilizer, may be abundant in carbonatitic systems.

4.3 Whole-rock geochemistry

Whole-rock geochemical data are available in Enclosure 4.3 in excel spreadsheet format. Table 3 presents a summary of the geochemical data for both LHKB-1 and LHKB-2 and will be discussed below.

A total of 1522 samples were analysed for whole-rock composition. Nearly every metre of core LHBK-1 has been analysed, which corresponds to 989 analyses; whereas 533 analyses were performed on LHBK-2. Early logging of the cores made it clear that the second core (LHBK-2) contains large sections of damtjernite breccia, a rock type barren in terms of REE. The damtjernite parts of the core were therefore not analysed.

Core ID	Average	Median	Mode	Minimum value	Maximum value
TRE_2O_3 (wt%)					
LHKB-1	1.19	1.08	1.10	0.02	10.17
LHKB-2	1.79	1.70	1.75	0.06	5.18
Ce (ppm)					
LHKB-1	4849.5	4360	3080-3700	85	42100
LHKB-2	7439.6	7020	8440	235	21900
Nd (ppm)					
LHKB-1	1521.2	1355	1050	23.7	10350
LHKB-2	1972.6	1845	1275	95.6	5660
Dy (ppm)					
LHKB-1	16.4	13.5	13.8	0.8	96.8
LHKB-2	12.8	11.6	10.1-10.7	1.5	66.6
Th (ppm)					
LHKB-1	233.2	181.5	216	4.8	2150
LHKB-2	159.7	128.5	110.5	11.1	1255
Ba (ppm)					
LHKB-1				50	>10000
LHKB-2				60	7740
P (ppm)					
LHKB-1				130	>10000
LHKB-2				70	>10000

Table 3: Average, median, mode, minimum and maximum values of TRE_2O_3, Ce, Nd, Dy, Th, Ba and P

4.3.1 Geochemistry of LHKB-1

The distribution of the Total Rare Earth Oxide (TR_2O_3) versus depth is presented in figure 11. All lanthanides (La to Lu) were calculated as Total Rare Earth Oxides (TRE_2O_3) weight percent using the following formula:

$$La_2O_3 \text{ (wt\%)} = \frac{La \text{ (ppm)} * \text{(atomic Mass La *2)}}{\text{(Atomic mass } La_2O_3\text{)}} / 10000$$

$$TR_2O_3 \text{ (wt\%)} = La_2O_3 + Ce_2O_3 + Pr_2O_3 + Nd_2O_3 + Sm_2O_3 + Eu_2O_3 + Gd_2O_3 + Tb_2O_3$$
$$+ Dy_2O_3 + Ho_2O_3 + Er_2O_3 + Tm_2O_3 + Yb_2O_3 + Lu_2O_3$$

Rare Earth Elements are present throughout LHKB-1. However, the concentration of TR_2O_3 is highly variable (0.02 to 10.17 wt%-Table 3) with three individual metres containing more than 5 wt% TR_2O_3 (Fig. 11).

The average TR_2O_3 for LHKB-1 is 1.19 wt% with most of the samples containing between 0.8 and 1.6 wt% (Fig. 12).

Rare Earth Element patterns of the LHKB-1 samples are presented in figure 13. Fe-dolomite carbonatite is enriched in LREE, as expected, and display steep REE patterns with little to no Eu anomaly. Cerium (Ce) is the most abundant REE present with concentrations ranging from 85 to 42100 ppm (Table 3), followed by La and Nd. Neodymium concentrations ranges from 23.7 to 10350 ppm, whereas dysprosium (Dy) varies from 0.8 to 96.8 ppm. Note that the patterns for the most depleted in HREE are jagged. These elements are present in concentrations close to the detection limit, and in the lower part of the diagram where small variations in concentrations are emphasised due to the log scale. The most enriched samples contain concentrations of HREE up to 200 times chondrite (Fig. 13).

The distribution of elements of interest such as P, Ba, Th, Nd and Dy versus depth are plotted in Figure 14. Data for both barium and phosphorus are limited by the analytical method which is calibrated for concentrations up to 10000 ppm. Only one sample is concerned for Ba, however 10.3 % of the samples (102 samples) contain more than 10000 ppm P. The concentration of thorium is relatively low with a median of 181.5 ppm. Concentrations of neodymium and Dysprosium range from 23.7 to 10350 ppm and 0.8 to 96.8 ppm respectively.
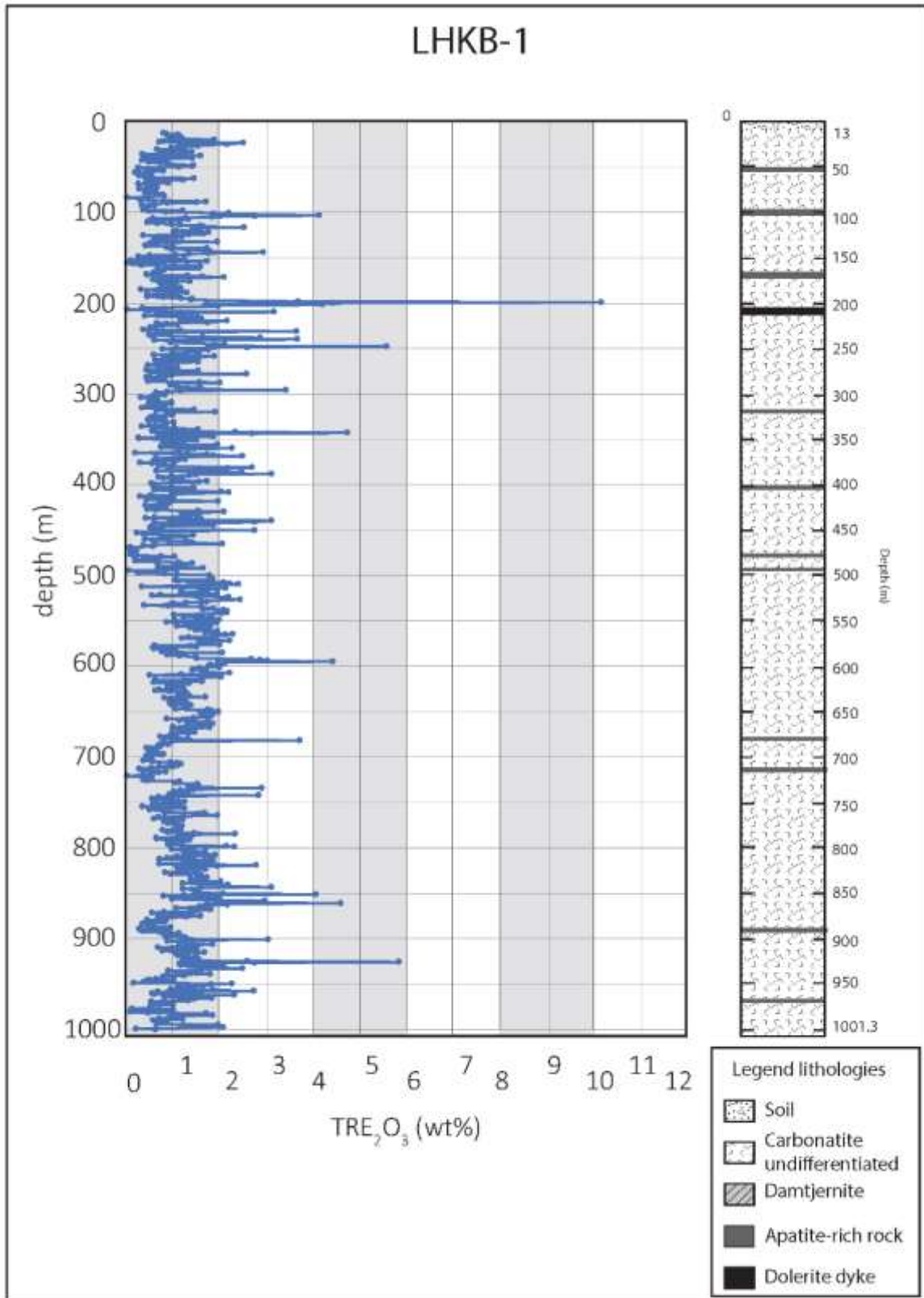
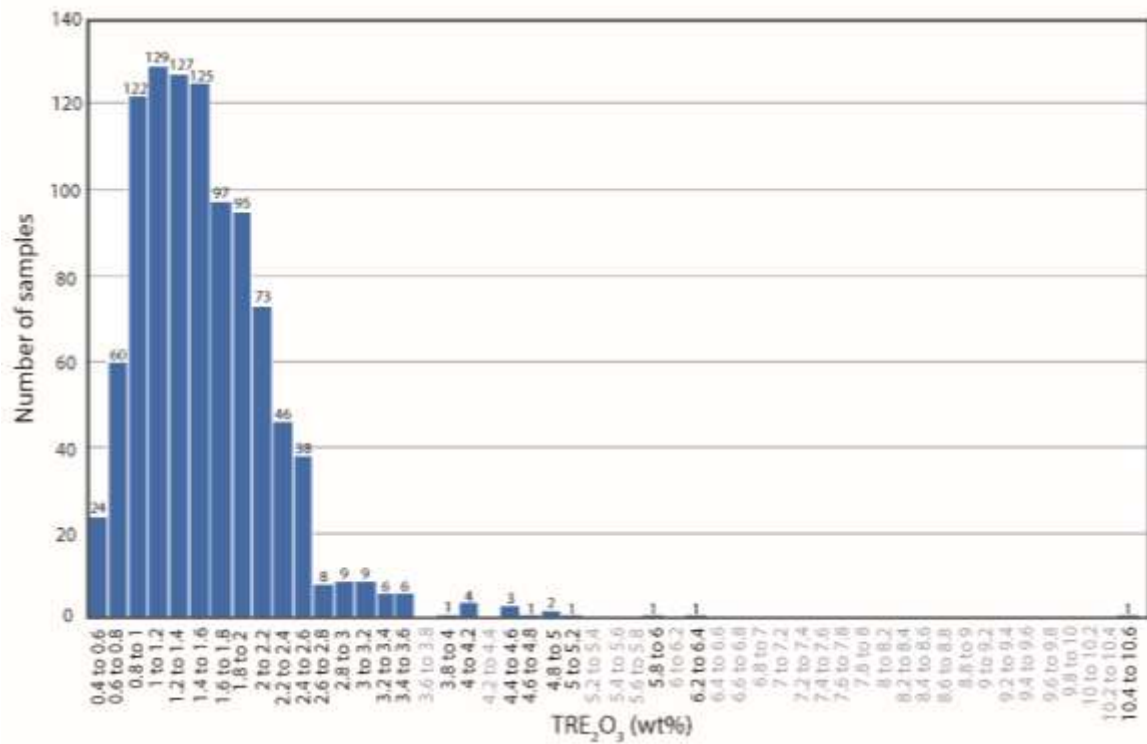*Figure 11: Total of Rare Earth Oxide in weight percent in LHKB-1.*

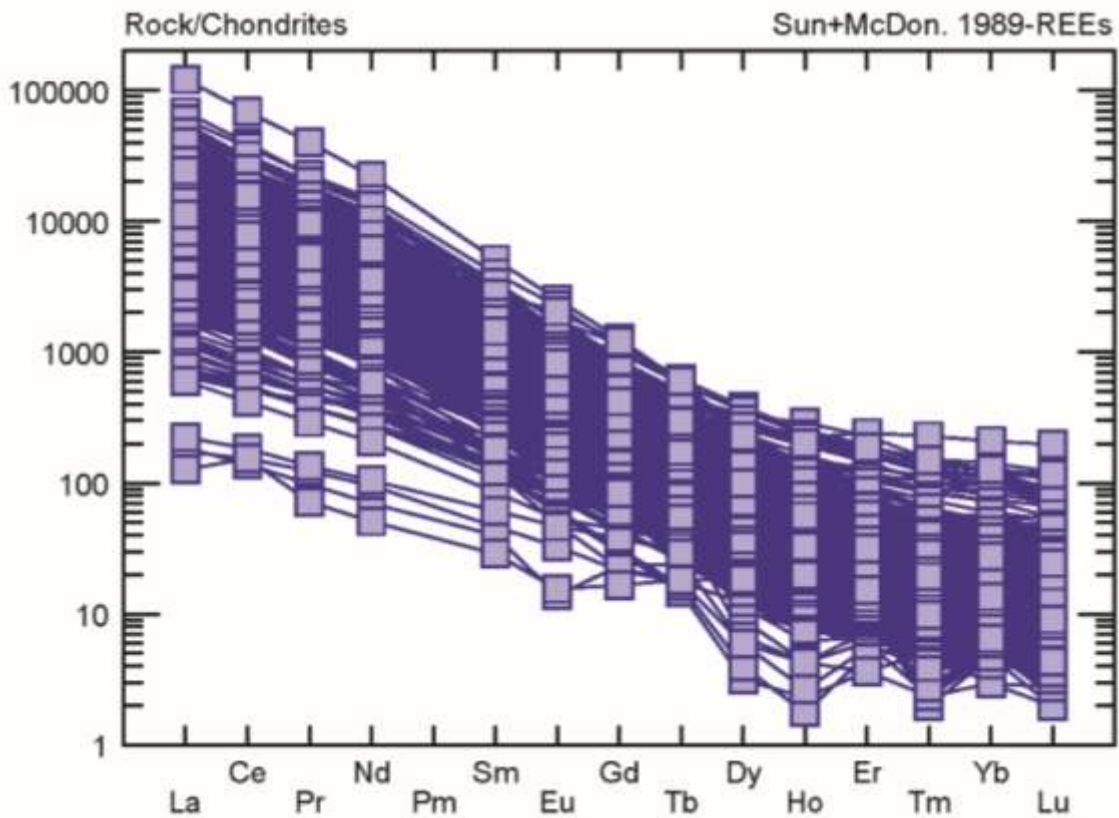*Figure 12: Distribution of TRE₂O₃ (wt%) in LHBK-1.*

Figure 13: Chondrite normalize REE diagram of samples from LHKB-1. Note the strong enrichment in LREE.
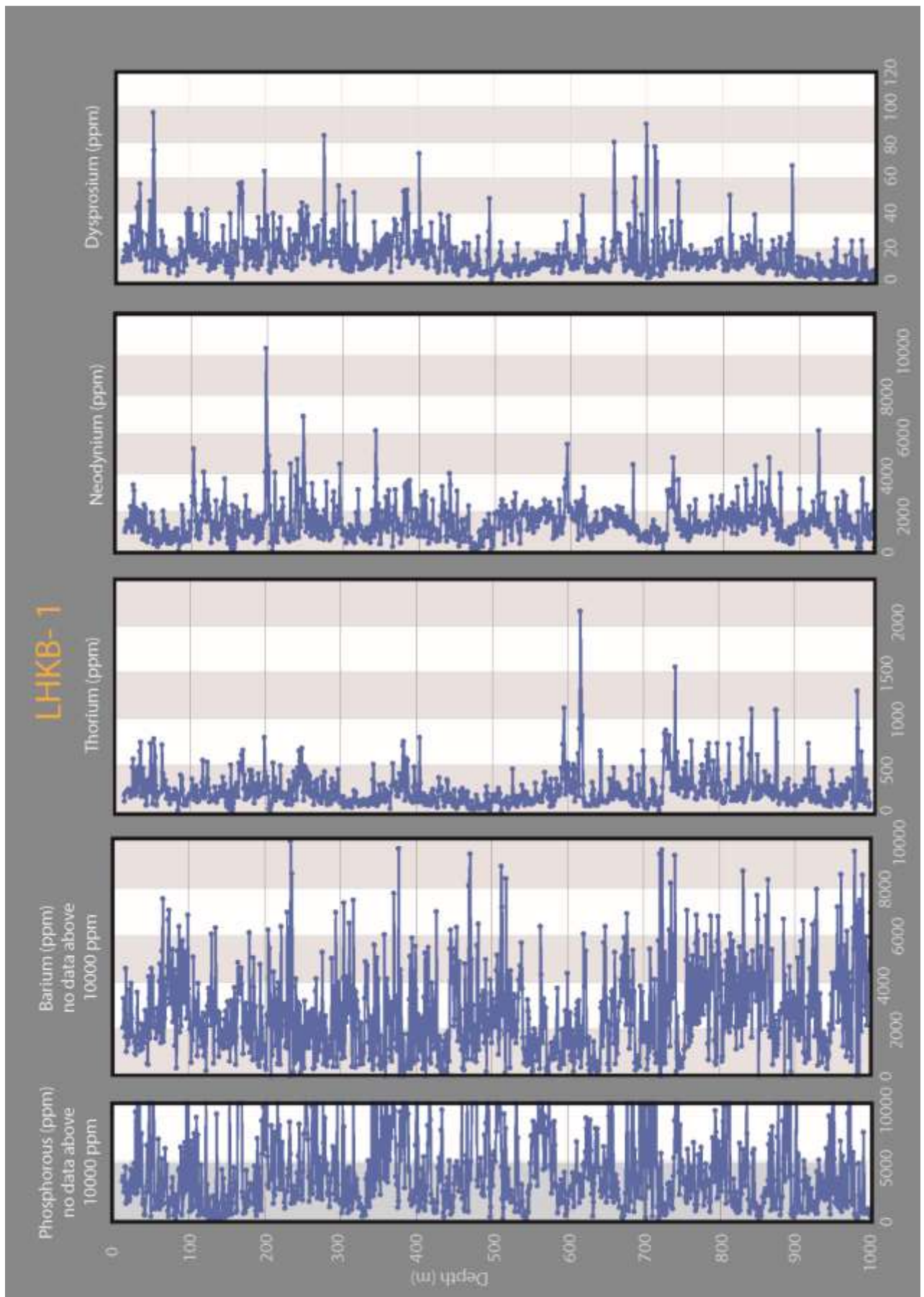
Figure 14: Distribution of P, Ba, Th, Nd and Dy as a function of depth in LHKB-1.

4.3.2 Geochemistry of LHKB-2

The second core, LHKB-2, contains overall a higher content of TRE_2O_3 than LHKB-1 with an average of 1.79 wt% (Table 3), although, as in LHKB-1, the REE content varies from one sample to the next. Two samples contain more than 5 wt % TRE_2O_3. Two zones with slightly elevated concentration in REE can be defined: one located from 13 to 200 m and a second from 500 to 700 m, where many samples contain between 1 and 4 wt% TRE_2O_3 (Fig. 15).

278 samples contain between 1 and 2 wt% TRE_2O_3 and represent 52,1 % of the samples (Fig. 16).

Samples from LHKB-2, like the one in LHKB-1, are also strongly enriched in LREE and particularly in Ce (Fig. 17). Some samples display a pattern flattening out towards the HREE which can reach up to 100 times chondrite. The samples do not display any obvious Eu anomalies.

A few other elements are plotted against depth (Fig. 18). Barium concentrations vary between 50 and 7740 ppm. Phosphorus concentrations are highly variable and varies from 60 ppm to more than 10000 ppm. Proportionally, LHKB-2 contain less samples above 10000 ppm P than LHKB-1; 7.7 % versus 10.3 %. The distribution of Th is relatively homogeneous, and the amount of Th remains low (median: 128.5 ppm), although a few samples (<10) contain more than 500 ppm Th. The trend displayed by Nd is similar to the one displayed by TRE_2O_3 (Fig. 15), which indicates that Nd behaved like a LREE in the system. Dysprosium concentrations are low with most samples containing less than 20 ppm (Fig. 18).
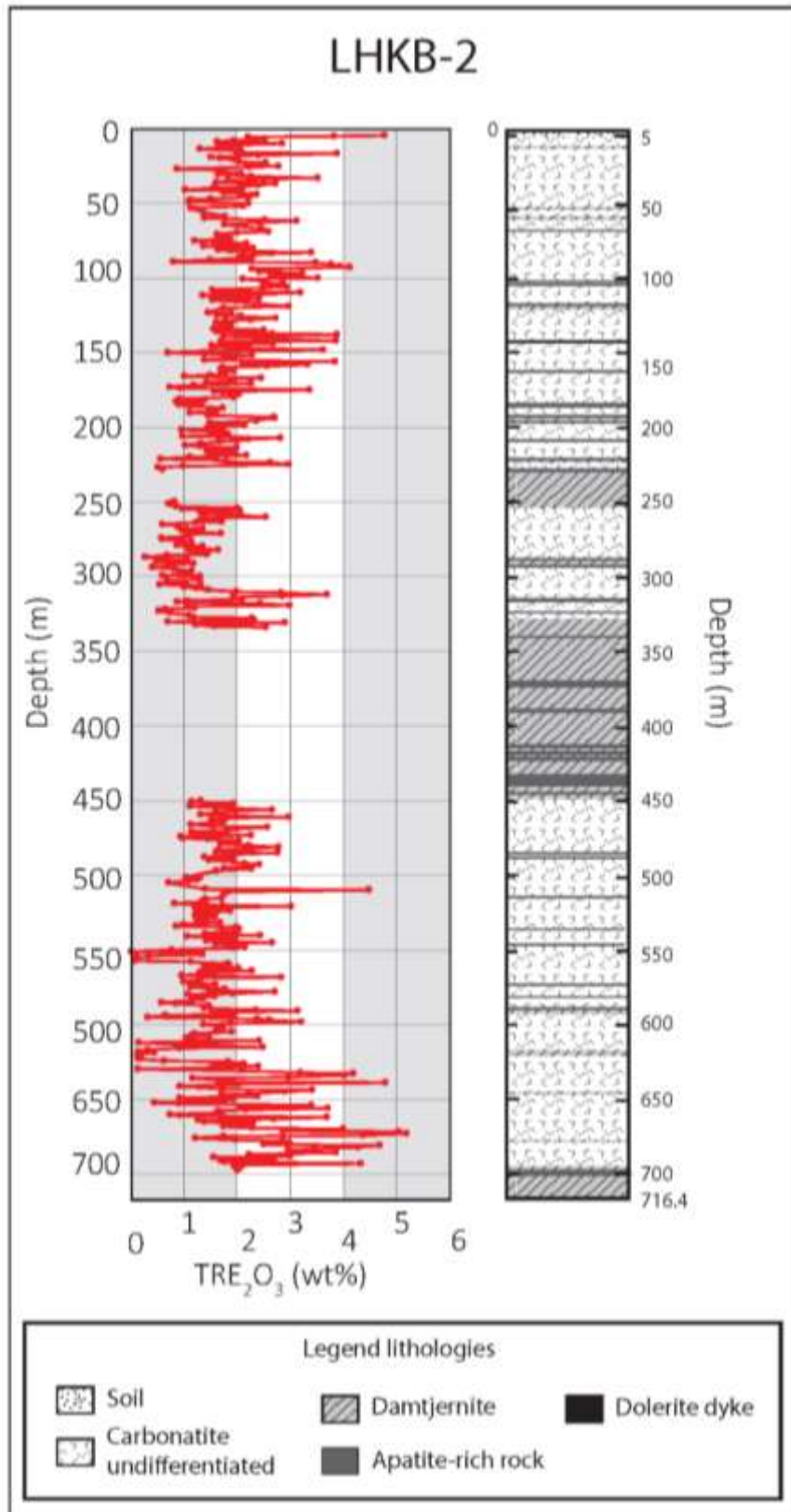
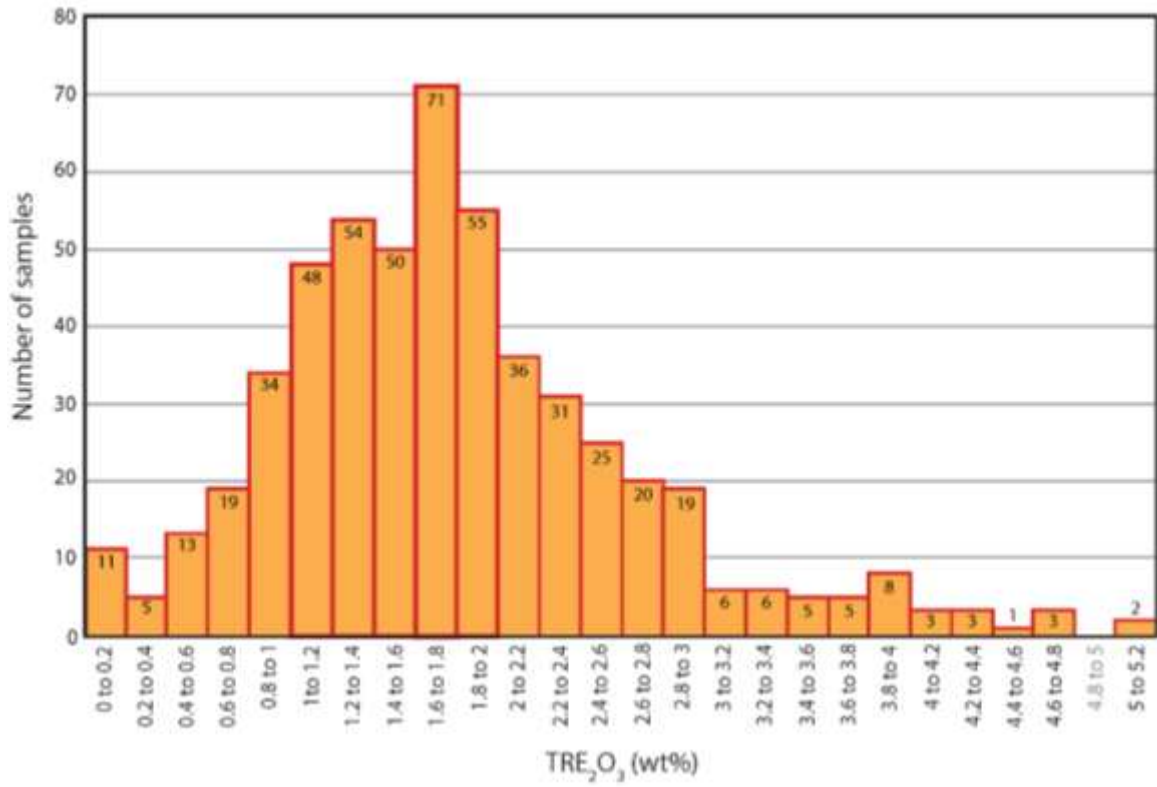*Figure 15: Total Rare Earth Oxide in weight percent in LHKB-2.*

29

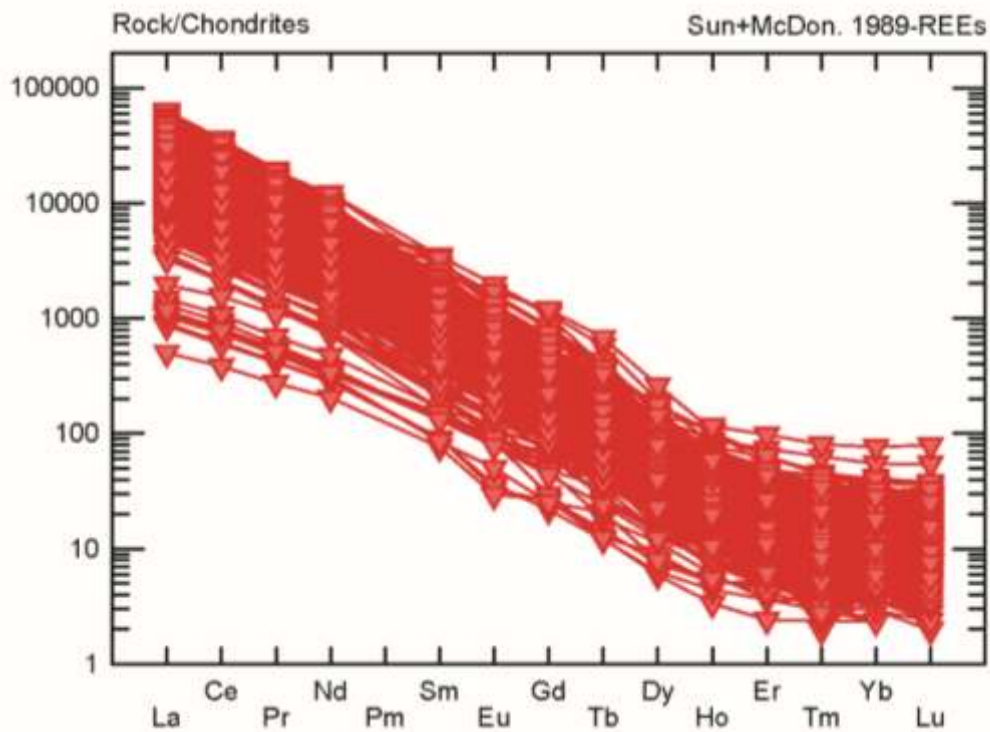*Figure 16: Distribution of TRE₂O₃ (wt%) in LHBK-2.*

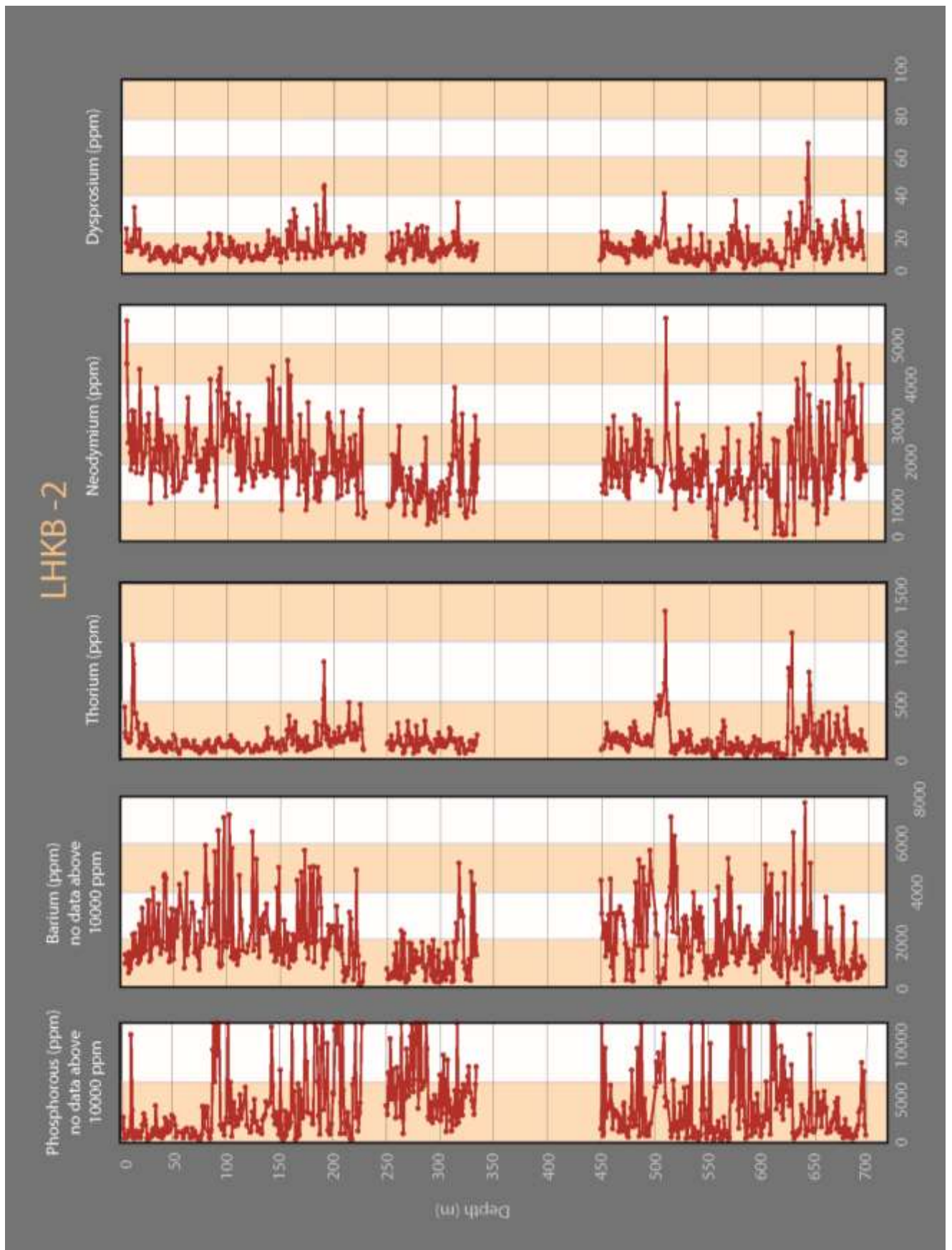*Figure 17: REE pattern of the LHKB-2 samples.*

Figure 18: Distribution of P, Ba, Th, Nd and Dy as a function of depth in LHKB-2.

31

4.4 Mineralogy and microtextural relationships

4.4.1 Mineralogy

The mineralogy and textural relationships of the REE-minerals in the Fe-dolomite carbonatite at Fen are described, based on observations of two cores, and rocks coming from the same unit previously studied (Schilling, 2013) and analysed by SEM and microprobe.
By visual inspection of the LHKB-cores, using a hand-lens, a binocular microscope and a hand-held XRF, and comparing with what is known from other samples, the following minerals represent the typical minerals in the cores: The processing possibilities are not assessed here.

Major minerals include Fe-dolomite, chlorite/mica, barite, pyrite/pyrrhotite, magnetite/(hematite), apatite and quartz. Minor phases comprise thorite, allanite, sphalerite, galena, chalcopyrite, fluorite and "columbite" (the latter probably is an alteration product of pyrochlore in søvite xenoliths). Evidently, alkali-feldspar is present in places, most likely as Ba-bearing/Ba-rich varieties. The REE-minerals are parisite-synchysite, bastnaesite and monazite. These minerals are generally very fine-grained, but typically occur in sizeable clusters (from mm-size to cm and dm size). These clusters vary in colour: red, brown, brownish-gray, orange, yellow etc.

4.4.2 REE-mineral clusters

The carbonatites display a wide range of textures and the mineral assemblages can vary on mm-scale. The example shown below illustrate one of the observed mineral assemblages and its associated texture.

As shown by the geochemical diagrams (Fig. 5, 6, 15 & 18), REE-minerals are not evenly distributed throughout the cores but rather tend to form clusters with other minerals in the carbonatite (Fig. 19). The example chosen below is one of the areas where the largest cluster of REE-minerals are found in LHKB-1 (Fig. 5D). There REE-minerals are clearly detected by hyperspectral imaging (Fig. 10). Back-scattered Electron (BSE) imaging, enhancing atomic weight variations between various minerals, illustrates the distribution of minerals in the rocks. The brighter the colour, the heavier the mineral. Therefore, REE-minerals but also barite and thorite appear bright, whereas carbonates are darker. Energy Dispersive X-ray spectroscopy (EDS) maps show the distribution of various chemical elements (Fig. 19 F to I). REE-mineralizations, which are mainly composed of LREE-rich carbonates (bastnaesite and parasite/synchisite), are associated with barite and zoned dolomite with Mg-rich cores and Ca-rich rims. Accessory thorite ($ThSiO_4$) is dispersed in the mineralization. Note that REE-bearing carbonates cannot be identified using EDS maps alone.
Other REE-mineral clusters indicate that REE carbonate(s) and fluorocarbonates can be associated with intergrown fine-grained monazite, a LREE phosphate.

Future investigation of the core will focus on the characterization of minerals and textures in the different rock types and including a full characterization of the REE-minerals (Dahlgren, in prep).
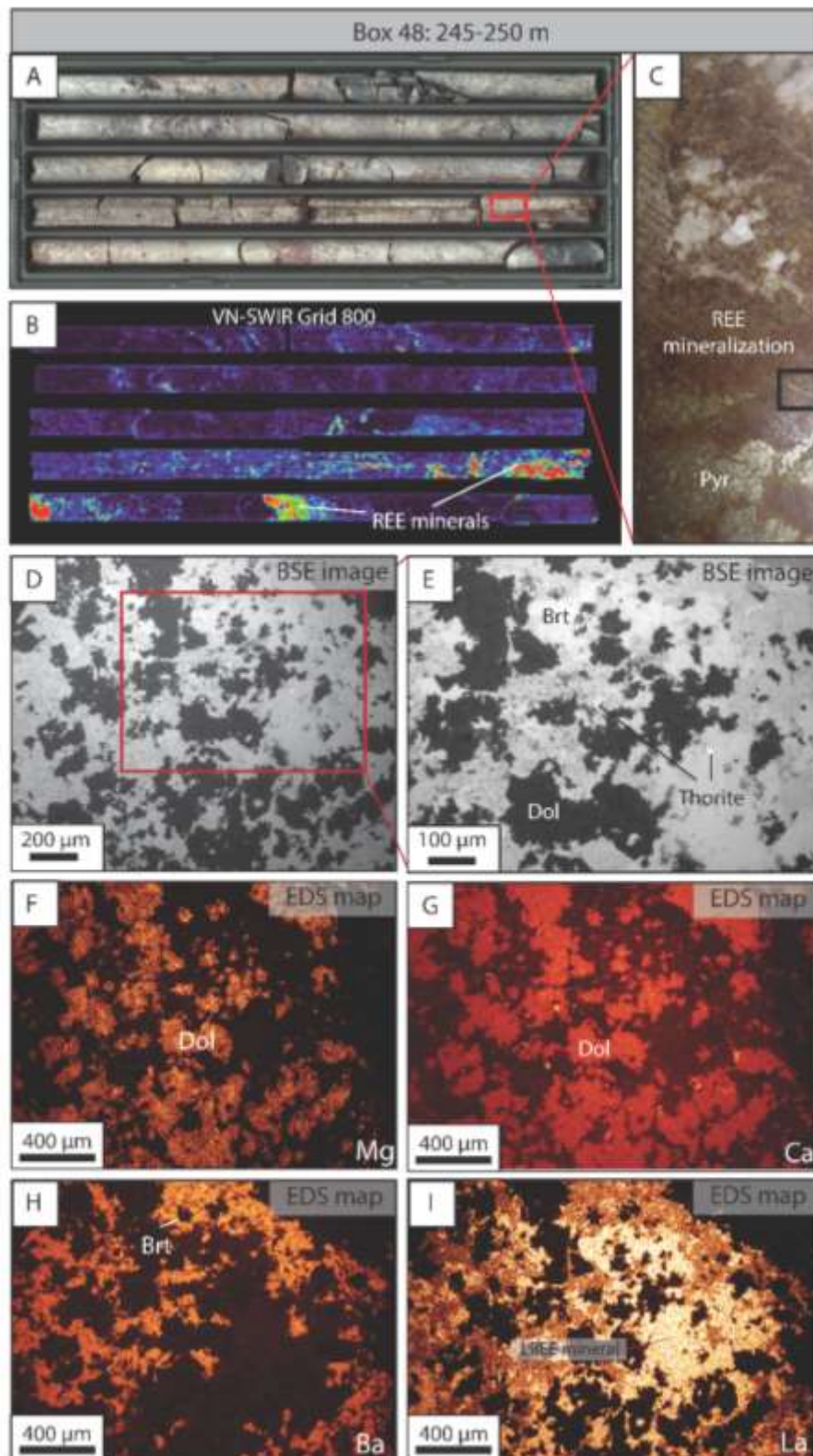

Figure 19: Texture of REE-mineralizations. A. Photo of the core box and location of the sample presented in this figure. B. Near Visible SWIR Grid 800 enhancing the location of REE-minerals in the core. D & E. Back Scattered Electron images of area mapped using EDS below. F to I: Energy Dispersive X-ray Spectroscopy maps showing chemical variation in the area presented in D.

5. CONCLUSION

- This report is a data repository for the two new reconnaissance drill-cores, LHKB-1 and LHKB-2, in the REE-bearing Fe-dolomite carbonatite of the Fen Complex.
- Hyperspectral imaging is available for both cores and 1522 whole-rock analyses of one-metre intervals have been produced.
- Hyperspectral imaging is highly relevant for studying carbonatites. Identification and localization of various rock-types, abundance and chemical variations of carbonates are easily extracted from the dataset.
- Both cores are dominated by Fe-dolomite carbonatite which document that the REE-enriched carbonatite continues at depth.
- LHKB-1 is mainly composed of Fe-dolomite carbonatite with thin apatite-rich layers. Damtjernite (chlorite-bearing lamprophyre) is only encountered locally. A one-metre-thick dolerite dyke associated with the Oslo rift has also been encountered. Total Rare Earth Oxide in the core averages at 1.19 wt% based on 989 analyses.
- LHKB-2, is also composed predominantly of Fe-dolomite carbonatite but also contains several thick intervals of damtjernite (lamprophyre), up to 115 m thick. Overall, LHKB-2 is characterized by a higher content of TRE_2O_3 than LHKB-1, with an average of 1.79 wt%, for 533 samples.
- The main REE-minerals encountered in the cores are REE carbonate (bastnäsite) and REE fluorocarbonate (parasite/synchisite). Monazite and allanite have also been observed in some samples. Mineral assemblage and textures remain to be examined in more details and will be the focus of subsequent studies. The results presented here indicate that the Fe-dolomite carbonatite continues to more than one-thousand-metre depth and that it contains relatively abundant REE-mineralizations.

References

Andersen, T. (1984). Secondary processes in carbonatites: petrology of "rødberg" (hematite-calcite-dolomite carbonatite) in the Fen central complex, Telemark (South Norway). *Lithos* **17**, 227-245.

Andersen, T. (1986). Magmatic fluids in the Fen carbonatite complex, S.E. Norway: Evidence of mid-crustal fractionation from solid and fluid inclusions in apatite. *Contributions to Mineralogy and Petrology* **93**, 491-503.

Andersen, T. (1987). Mantle and Crustal Components in a Carbonatite Complex, and the Evolution of Carbonatite Magma - Ree and Isotopic Evidence from the Fen Complex, Southeast Norway. *Chemical Geology* **65**, 147-166.

Andersen, T. (1989). Carbonatite-Related Contact Metasomatism in the Fen Complex, Norway - Effects and Petrogenetic Implications. *Mineralogical Magazine* **53**, 395-414.

Brøgger, W. C. (1921). Die eruptivgesteine des Kristianiagebietes, IV. Das Fengebiet in Telemark, Norwegen. *Det Norske Videnskaps Akademi i Oslo, Matematisk-naturvitennskapelig klasse 1920* **9**.

Dahlgren, S. (1983). Naturlig radioaktivitet i berggrunnen, gammastralingskart, Fensfeltet, Telemark, scale 1:10,000. 'Prosjekt temakart, Telemark'.

Dahlgren, S. (1987). The satellitic intrusions in the Fen carbonatite alkaline rock province, Telemark, Southeastern Norway. University of Oslo, 298.

Dahlgren, S. (1994). Late proterozoic and Carboniferous ultramafic magmatism of carbonatitic affinity in southern Norway. *Lithos* **31**, 141-154.

Dahlgren, S. (2004). Nordagutu, 1713 IV. *1:50 000 Bedrock map*: Geological Survey of Norway.

Dahlgren, S. (2006). Fenvulkanen In: Ramberg, I. B., Bryhni, I. & Nøttvedt, A. (eds.) *Landet blir til*: Norges geologi, 146.

Dahlgren, S. (2008). Thorium i Buskerud, Telemark og Vestfold fylker. Buskerud, Telemark og Vestfold fylker, 20.

Dahlgren, S. (2012). Thorium i Fensfeltet-ressursanslag. Buskerud, Telemark og Vestfold fylkeskommuner, 24.

Dahlgren, S. (2015). REE and thorium potential of the Fen Complex. . *Norway – A supplement to Mining Journal*, 12.

Davris, P., Marinos, D., Balomenos, E., Alexandri, A., Gregou, M., Panias, D. & Paspaliaris, I. (2018). Leaching of rare earth elements from 'Rödberg' ore of Fen carbonatite complex deposit, using the ionic liquid HbetTf2N. *Hydrometallurgy* **175**, 20-27.

Goodenough, K. M., Schilling, J., Jonsson, E., Kalvig, P., Charles, N., Tuduri, J., Deady, E. A., Sadeghi, M., Schiellerup, H., Muller, A., Bertrand, G., Arvanitidis, N., Eliopoulos, D. G., Shaw, R. A., Thrane, K. & Keulen, N. (2016). Europe's rare earth element resource potential:

An overview of REE metallogenetic provinces and their geodynamic setting. *Ore Geology Reviews* **72**, 838-856.

Griffin, W. L. (1973). Lherzolite nodules from the Fen alkaline complex, Norway. *Contributions to Mineralogy and Petrology* **38**, 135-148.

Heincke, B. H., Smethurst, M. A., Bjørlykke, A., Dahlgren, S., Rønning, J. S. & Mogaard, J. O. (2008). Airborne gamma-ray spectro-meter mapping for relating indoor radon concentrations to geological parameters in the Fen region, southeast Norway. In: Slagstad, T. (ed.) *Geological Survey of Norway Special Publication*, 131-143.

Krasnova, N. I., Petrov, T. G., Balaganskaya, E. G., Garcia, D., Moutte, J., Zaitsev, A. N. & Wall, F. (2004). Introduction to phoscorites: occurence, composition, nomenclature and petrogenesis. In: Wall, F. & Zaitsev, A. N. (eds.) *Phoscorites and Carbonatites from MAntle to Mine: the key example of the Kola Peninsula*: Mineralogical Society of Great Britain & Ireland, 45-74.

Neave, D. A., Black, M., Riley, T. R., Gibson, S. A., Ferrier, G., Wall, F. & Broom-Fendley, S. (2018). On the Feasibility of Imaging Carbonatite-Hosted Rare Earth Element Deposits Using Remote Sensing*. *Economic Geology* **111**, 641-665.

Paulick, H. & Machacek, E. (2017). The global rare earth element exploration boom: An analysis of resources outside of China and discussion of development perspectives. *Resources Policy* **52**, 134-153.

Sæther, E. (1957). The alkaline rock province of the Fen Area in southern Norway. *Det Kgl. Nor. Vidensk. Selsk. Skr.1957*. Trondheim, 148.

Schilling, J. (2013). Petrography, mineralogy and whole-rock data of the major lithologies of the Fen complex. In: NGU (ed.) *NGU report*: NGU, 18.

Svinndal, S. (1971). Undersøkelser etter sjeldne jordartsmetaller (RE) i Fensfeltet, Ulefoss, Nome, Telemark. NGU rapport, 1-18.

Svinndal, S. (1973). Thorium i Fensfeltet. *NGU Report*: NGU, 28.

Tse, P.-K. (2011). China's rare-earth industry. *U.S. Geological Survey Open-File Report*, 11.

Turner, D. J., Rivard, B. & Groat, L. A. (2014). Visible and short-wave infrared reflectance spectroscopy of REE fluorocarbonates. *American Mineralogist* **99**, 1335-1346.

USGS. (2011). Critical Materials Strategy. U.S. Department of Energy, 190.

Verplanck, P. L., Van Gosen, B. S., Seal, R. R. & McCafferty, A. E. (2014). A deposit model for carbonatite and peralkaline intrusion-related rare earth element deposits. *U.S. Geological Survey Scientific Investigations Report*: USGS, 58.

Vogt, J. H. L. (1918). Jernmalm og jernverk. *NGU-bulletin* **85**, 1-181.